

Interactive comment on “Mesoscale modeling study of the interactions between aerosols and PBL meteorology during a haze episode in China Jing-Jin-Ji and its near surrounding region – Part2: Aerosols’ radiative feedback effects” by H. Wang et al.

Anonymous Referee #2

Received and published: 21 January 2015

The paper addresses the radiative feedback on radiation budget, PBL meteorology and haze formation due to aerosols during the haze episode in China Jing-Jin-Ji and its nearby surrounding region using GRAPES-CUACE/haze model. I believe this manuscript is appropriate for publication in ACP and would recommend publication subject to primarily minor revisions outlined below.

- 1) How reliable is the analysis about the interactions between aerosols and PBL meteorology in a case study (5-day)? Could you please estimate or discuss the uncertainty of results in the paper? This is my biggest concern.

Response:

It is very difficult to test the reliability of the interactions between aerosols and PBL meteorology exactly because there are not direct observation results to compare with simulation results. However, we can control the uncertainties by evaluating the errors of key aerosols’ radiative parameters (AOD, SSA and ASY) to determine the radiative feedback. In fact, the model errors and evaluation of these three parameters are given in the companion paper “Mesoscale modeling study of the interactions between aerosols and PBL meteorology during a haze episode in China Jing-Jin-Ji and its near surrounding region – Part1: Aerosol distributions and meteorological features ” and we think the simulated results are reasonable. Further, the radiative transfer model developed by the Climate and Radiation Branch, NASA/Goddard Space Flight Center (the CLIRAD_SW and CLIRAD_LW) (Chou et al., 1998, 2001), which are widely used in the aerosol-radiation research, are used in this study.

Nevertheless, the results in this paper are only from a case study and more cases are needed to further simulation to verify the result. This is pointed out in the section 6 Discussion and conclusion.

- 2) The paper said “Based on official information about national emission sources in 2006 (Cao et al., 2006), the detailed high-resolution emission inventories of reactive gases, i.e. SO₂, NO_x, CO, NH₃ and VOCs, from emissions over China in 2007 were updated to form the current emission data (Cao et al., 2010). How to calculate the anthropogenic aerosol emission over China in 2008? More details about emission inventory should be mentioned.

Response:

Emission inventory collection is a very complex and hard work process. Normally, anthropogenic gas and aerosol emission inventory data collection is postponed 2-3 years. It is acceptable that emission data used by model is updated every two or three years. Emission data based on 2006 and 2007 are used in this paper.

The emission related content are introduced in brief in “Mesoscale modeling study of the interactions between aerosols and PBL meteorology during a haze episode in China Jing-Jin-Ji and its near surrounding region – Part1: Aerosol distributions and meteorological features ”. The detailed description of the emission data used here is introduced in the three papers (Cao, et al., 2006; 2010; An et al., 2013).

An, X. Q., Sun, Z. B., Lin, W. L., Jin, M., and Li, N.: Emission inventory evaluation using observations of regional atmospheric background stations of China, *J. Environ. Sci.*, 25, 537–546, 2013.

Cao, G., Zhang, X., and Zheng, F.: Inventory of black carbon and organic carbon 446 emissions from China, *Atmos. Environ.*, 40, 6516–27, 2006.

Cao, G. L., An, X. Q., Zhou, C. H., Ren, Y. Q., and Tu, J.: Emission inventory of air pollutants in China, *Chin. Environ. Sci.*, 30, 900–906, 2010.

3) Please improve all figures in the paper including quality, color bar, words and units. . . .

Response:

All figures are red-drawn.

4) How to define and calculate the turbulence diffusion coefficient (FKTM) in the paper? More detail information should be mentioned.

Response:

The turbulence diffusion coefficient (fktm) appears first time in “Mesoscale modeling study of the interactions between aerosols and PBL meteorology during a haze episode in China Jing-Jin-Ji and its near surrounding region – Part1: Aerosol distributions and meteorological features ”. It parameterizes the PBL turbulence diffusion process and the definition is given in another paper (Wang et al., 2010).

Wang, H., Zhang, X. Y., Gong, S., Chen, Y., Shi, G., and Li, W.: Radiative feedback of dust aerosols on the East Asian dust storms, *J. Geophys. Res.*, 115, D23214, doi:10.1029/2009JD013430, 2010.

Interactive comment on “Mesoscale modeling study of the interactions between aerosols and PBL meteorology during a haze episode in China Jing-Jin-Ji and its near surrounding region-Part2: Aerosols’ radiative feedback effects” by H. Wang et al.

Anonymous Referee #1

Received and published: 13 December 2014

This paper uses the chemical weather model GRAPES_CUACE with online aerosol radiation scheme to study the interactions between aerosols and meteorology during a haze episode in Eastern China. The authors show that synthetic impacts of aerosols’ radiative feedback effects result in about a significant increase in surface PM_{2.5} for haze events. The analysis is sound and the results are well presented. I only have few minor concerns. Overall, I recommend the paper for publication in ACP after the authors address following comments:

1) Page 28271, line 3: The acronym RAD at the first time in the paper should be explained.

Response:

A experiment means s simulation with online aerosol-radiation (RAD) interactions , this is revised in the manuscript.

2) Page 28272, line 6-7: Please clarify and correct “a sequence that has been widely noted and studied”.

Response:

It should be”...which has been widely ...” and this has been revised in the manuscript.

3) Page 28272, line 11: Please add “in the lower troposphere” after “meteorological conditions”

Response:

It is revised in the manuscript.

5) Page 28274, line 12: Please change “Where l” to “Where i ”

Response:

It is revised in the manuscript.

5) Page 28278, line 5-7: Please give some interpretation about “Points A, B, and C lie offshore of the Chinese coast, their temperature changes and those within SEA1 (Fig. 3d) being quite different from those within the LAND region. Why do the different and even opposite changes in vertical temperature profile induced from aerosols’ radiative feedback effects exist between land and sea regions”?

Response:

These phrases are revised as the following in the manuscript:

Points A, B, and C lie offshore of the Chinese coast and SEA1 represents the near China Sea region. The vertical temperature changing profiles induced from aerosols’ radiative feedback effect over those are quite different from those over the LAND region due to the different surface albedo and the height and depth of aerosols layer.

6) Page 28280, line 24: Please change “to the west” to “in the western edge”.

Response:

It is revised in the manuscript.

7) Table 1: Are DT06 and DP06 the difference in air temperature and pressure between RAD and CTL experiments or the weighing coefficient? Please check!

Response:

DT06/DP06 is air temperature (K) /surface pressure (hPa) differences between RAD and CTL experiments in Table 1.

8) The caption of Figure 1 should be “Figure 1. The averaged MODIS (top) and modeled AOD (bottom)”

Response:

They are revised in the manuscript.

9) Figures 3a and 3b: both color scale bars are overlaid. Please correct.

Response:

All figure3 are redrawn. This is revised in Figure 3.

10) The caption of Figure 7 should be corrected with “Figure 7. The PBL averaged air pressure (Pa) from the CTL experiment (top) and its difference between the RAD and CTL experiments (bottom) of 7–11 July.” . Please note the unit.

Response:

It is revised in the manuscript including the hPa unit.

11) The quality of some figures is poor, the colors, number and words are hard to identify. Please improve the figures.

Response:

All the figures are examined and most of them are re-drawn.

1 **Mesoscale modeling study of the interactions between**
2 **aerosols and PBL meteorology during a haze episode in**
3 **China Jing-Jin-Ji and its near surrounding region:**

4 **Part 2. Aerosols' radiative feedback effects**

5 **H. Wang^{1,2*}, G. Y. Shi³, X. Y. Zhang¹, S. L. Gong¹, S. C. Tan³, B. Chen³,**
6 **H. Z., Che¹, T. Li⁴**

7 1 Institute of Atmospheric Composition, Key Laboratory of Atmospheric
8 Chemistry (LAC) of China Meteorological Administration (CMA), Chinese
9 Academy of Meteorological Sciences (CAMS), Beijing, 100081, China

10 2 Collaborative Innovation Center on Forecast and Evaluation of
11 Meteorological Disasters, Nanjing University of Information Science &
12 Technology, Nanjing 210044, China

13 3 State Key Laboratory of Numerical Modeling for Atmospheric Sciences
14 and Geophysical Fluid Dynamics (LASG), Institute of Atmospheric
15 Physics, Chinese Academy of Sciences, Beijing, 100029, China

16 4 School of Atmospheric Physics, Nanjing University of Information Science
17 & Technology, Nanjing 210044, China

18

19 Corresponding author: wangh@cams.cma.gov.cn; wangh@rays.cma.gov.cn

20

21
22

Abstract

23 Two model experiments, namely a control (CTL) experiment without
24 aerosol-radiation feedbacks and a ~~RAD~~ experiment with online aerosol-
25 radiation (RAD) interactions, were designed to study the radiative feedback on
26 regional radiation budgets, PBL meteorology and haze formation due to
27 aerosols during haze episodes over China Jing-Jin-Ji and its near
28 surroundings (3JNS Region, for Beijing, Tianjin, Hebei Province, East Shanxi
29 Province, West Shandong Province and North Henan Province) with a two-
30 way atmospheric chemical transport model. The impact of aerosols on solar
31 radiation reaching Earth's surface, outgoing longwave emission at the top of
32 the atmosphere, air temperature, PBL turbulence diffusion, PBL height, wind
33 speeds, air pressure pattern and PM_{2.5} has been studied focusing on a haze
34 episode during the period from 7 to 11 July 2008. The results show that the
35 mean solar radiation flux that reaches the ground decreases about 15% in
36 China 3JNS Region and by 20 to 25% in the region with the highest AOD
37 during the haze episode. The fact that aerosol cools the PBL atmosphere but
38 warms the atmosphere above it leads to a more stable atmospheric
39 stratification over the region, which causes a decrease in about 52% of
40 turbulence diffusion and a decrease in about 33% of the PBL height. This
41 consequently forms a positive feedback on the particle concentration within
42 the PBL and the surface as well as the haze formation. On the other hands,
43 aerosol DRF (direct radiative forcing) increases about 9% of PBL wind speed,
44 weakens the subtropical high by about 14hPa, which aids the collapse of haze
45 pollution, resulting in a negative feedback to the haze episode. The synthetic
46 impacts from the two opposite feedbacks result in about a 14 % increase in
47 surface PM_{2.5}. However, the persistence time of both high PM_{2.5} and haze
48 pollution is not effected by the aerosol DRF. On the contrary over offshore
49 China, aerosols heat the PBL atmosphere and cause unstable atmospheric
50 stratification, but the impact and its feedback on the PBLH, turbulence
51 diffusion and wind is weak except its evident impacts on the subtropical high.

52

53
54

55 **1. Introduction**

56 Aerosol direct radiative forcing (DRF) arises from the reforming of the
57 Earth-atmosphere radiation budget by the absorption and scattering of solar
58 radiation, absorption and the emission of earth thermal radiation. This may
59 cool or heat the Earth-atmosphere system leading to the reforming of Earth-
60 atmosphere temperature profile followed by impacts on global and regional
61 climate, ~~a sequence that~~which has been widely noted and studied (*Hansen et*
62 *al., 1997; Ramanathan et al., 2001; Liao et al., 2006; Yu et al., 2006; Huang*
63 *et al., 2006a; 2006b; 2009; Che et al., 2014*).

64 Considering the short lifetime of most aerosol particles (about one week)
65 and their sharp uneven local and regional distribution and high dependence
66 on emission sources and local meteorological conditions in the lower
67 atmosphere (*Che et al., 2007, 2009; Huang et al., 2007; 2008; Wang et al.,*
68 *2014*), aerosol effects on smaller spatial and temporal atmospheric scales
69 may be worthy of greater attention. Studies at regional or local scales have
70 shown that the DRF due to aerosols can exceed, in terms of intensity, the
71 DRF attributable to greenhouse gases and lead to complex and important
72 feedback mechanisms at such scales (*Ramanathan, 2001; Li et al., 2007;*
73 *Shindell and Faluvegi, 2009*). The radiative feedback and impacts on
74 mesoscale weather due to aerosol DRF has caused widespread concern in
75 recent years. Certain studies have been conducted to simulate the impact on
76 mesoscale weather circulation, to evaluate the possible feedback on short
77 and medium-range weather and numerical prediction in different regions of
78 the world (*Grell et al., 2005; Fast et al., 2006; Perez et al., 2006; Wang et al.,*
79 *2006; Heinold et al., 2008; Chapman et al., 2009; Wang et al., 2010*).
80 However, current understanding of aerosol effects on weather contains major
81 uncertainties because the interactions among aerosols, meteorology,
82 radiation and chemistry are very complex and required to be studied in the
83 online coupled models.

84 Aerosols are the main pollutants when haze episodes occur in China and
85 PM₁₀ may reach up to 1000ug/m³ in China 3JNS Region (*Zhang et al. 2013;*
86 *Wang et al., 2014*) during severe, long-lasting hazy weather. Aerosol particles

87 suspended in local atmosphere lead to significant DRF and impacts on local
88 or regional circulation as well as on the developing process of hazy weather.
89 The meteorological condition of planetary boundary layer (PBL) has important
90 impacts on the occurrence, persistence, dissipation and pollution density of
91 the haze (*Vogelezang et al., 1996; Santanello et al., 2005, Cheng et al., 2002 ;*
92 *Pleim, 2007b*). Substantial aerosols may also influence PBL meteorology and
93 circulation and, evidently, in turn affect the haze and air pollution process by
94 its DRF since most aerosol particles concentrate in PBL during haze events.

95 Focusing on July 2008 and a haze episode from 7 to 11 July in China
96 3JNS Region, an external mixing scheme of 7 kinds of aerosols has been
97 introduced into the GRAPES-CUACE model to evaluate the optical features of
98 composite aerosols and discuss the PBL aerosol loading, the PBL
99 meteorological properties closely related to haze as well as their relationship
100 to haze episodes in a companion paper (Part 1). In this article, the aerosol
101 optical properties are used as input parameters in a radiative transfer scheme
102 where the radiative heating rates are online fed back to the dynamic frame of
103 the GRAPES_CUACE. This allow to evaluate aerosol DRF and its impact on
104 the local radiation budget and the PBL meteorological features including air
105 temperature, heating/cooling profile rates, wind intensity, planetary boundary
106 layer height (PBLH), turbulence diffusion, air pressure pattern over China
107 3JNS Region.

108 **2. Model Introduction**

109 The dynamic core, the physics processes option, the chemical frame
110 including emission sources, gas and aerosol processes and the interaction
111 between gas and aerosols in the GRAPES_CUACE model have been
112 introduced in Part 1. This section provides a brief description of the radiative
113 transfer scheme used in this research.

114 Several radiative transfer modes can be selected in the GRAPES-
115 CUACE model. The shortwave (SW) and longwave (LW) radiative transfer
116 models developed by the Climate and Radiation Branch, NASA/Goddard
117 Space Flight Center (CLIRAD_SW and CLIRAD_LW) (*Chou et al., 1998;*

118 2001) are used in this work for their convenience and fine capacity in
 119 processing aerosols (Wang et al., 2009; 2013). The CLIRAD includes the
 120 absorption due to water vapor, O₃, O₂, CO₂, clouds, and aerosols. Interactions
 121 among the absorption and scattering by clouds and aerosols are considered.
 122 The solar spectrum in the CLIRAD is divided into 11 bands and the thermal
 123 infrared spectrum into 10 bands from 3.333 to 40 μ m. For each atmospheric
 124 layer and spectral band, the effective optical thickness, single scattering
 125 albedo, and asymmetry factor are summed up over all gases and particles:

$$126 \quad \tau = \sum_i \tau_i \quad (1)$$

$$127 \quad \bar{\omega} = \sum_i \omega_i \tau_i / \sum_i \tau_i \quad (2)$$

$$128 \quad \bar{g} = \sum_i g_i \omega_i \tau_i / \sum_i \tau_i \omega_i \quad (3)$$

129 Where τ_i denotes ozone, water vapor, clouds, aerosols and atmospheric
 130 gases. Aerosols AOD (τ_a), SSA (ω_a) and ASY (g_a) are calculated by an
 131 external mixing scheme of different types of aerosols as described in the
 132 companion paper (Part 1). The effect of aerosols on solar and thermal
 133 radiation within the GRAPES-CUACE model is realized by implementing τ_a , ω_a ,
 134 and g_a into the CLIRAD radiation scheme. The radiative heating/cooling rates
 135 in the atmosphere, including aerosol absorption and scattering of solar and
 136 infrared radiation, were calculated and feedback to the thermal and dynamic
 137 processes at every radiation step in the GRAPES-CUACE model. The online
 138 active interaction of ‘meteorology-aerosol-radiation’ is completely achieved in
 139 the model and the radiative feedback on the local PBL as well as haze due to
 140 aerosols is studied using the model.

141 3. Experiment Design

142 The Control (CTL) experiment is the base simulation without calculating
 143 aerosol radiative feedback and impacts online as described in Part 1. In this
 144 paper, the simulation experiment (online active interacting meteorology-
 145 aerosol-radiation) is referred to as the RAD experiment. The only difference
 146 between the RAD and CTL experiments is that, in the RAD experiment, the

147 aerosol radiation heating/cooling effect is calculated online and feedback to
148 the model thermodynamic and dynamic processes.

149 In the following section, the simulation results of surface radiative fluxes
150 from the RAD experiment are compared with those of the CTL simulation as a
151 way to assess the aerosol impact on the local Earth-atmosphere radiation
152 balance. The differences between the RAD and CTL experiments concerning
153 the PBL meteorological fields, including PBL temperature, height, turbulence
154 diffusion, meteorological pattern and pollutant particle loading will be
155 discussed as part of the study of aerosol radiative effects and feedback on
156 local PBL thermal and dynamic processes. Finally, the aerosol impact on the
157 haze episode itself is discussed.

158 The haze episode occurred on 7-11 July 2008 was selected for this study.
159 All model configuration options and model parameters adopted were the
160 same as those used in the CTL experiment in Part 1. The initial fields and
161 lateral boundary data on the meteorology and tracers, together with the model
162 domain, horizontal and vertical resolution and both step and forecasting also
163 matched those used in the CTL experiment.

164 **4. The impacts on regional radiation budget**

165 The solar radiation flux reaching the Earth's surface may be changed
166 obviously due to aerosols absorbing and scattering of solar radiation during
167 the haze episode. A large numbers of particles suspended in the atmosphere
168 also launch infrared radiation and the outgoing longwave radiation at the top
169 of atmosphere (TOA) may be also changed. This leads to the reforming of
170 regional Earth-atmosphere radiation budget. The key factor impacting
171 radiation flux is the aerosol AOD. It can be seen in Figure 1 that the averaged
172 simulated AOD during 7 to 11 July shows an expected coherence with MODIS
173 Deep Blue AOD at 550 in horizontal distribution, affected area, peak values
174 and their geographical locations over China 3JNS Region and its downwind
175 area even though MODIS omits parts of the data in China 3JNS Region. The
176 land domain (111-119° E, 33-40° N named as LAND in Fig.1) with the highest
177 AOD values is regarded as the most representative of the China 3JNS region

178 where the aerosol impacts on meteorological fields are presented in the
 179 following sections. The three points labeled A (38.6° N, 119.5° E), B (35.0° N,
 180 120.7° E) and C (38.4° N, 122.0° E) in Figure1 are selected to represent
 181 China's offshore region. SEA1 (32.0 to 36.8° N, 121.5 to 126.0° E) denotes the
 182 sea area from the eastern coast of China ~~to-in~~ the west edge of the Korean
 183 peninsula, while SEA2 (30.0 to 42.0° N, 130.0 to 139.5° E) represents the sea
 184 area to the east of the Korean peninsula.

185 The percentage change in surface SW flux due to aerosol DRF at the
 186 surface (SFC) and change in LW at TOA are defined as:

$$187 \quad \Delta F_{SFC} = (Flux(\downarrow_{Solar,SFC})_{RAD} - Flux(\downarrow_{Solar,SFC})_{CTL}) / Flux(\downarrow_{Solar,SFC})_{CTL} \times 100\% \quad (4)$$

$$188 \quad \Delta F_{TOA} = (Flux(\uparrow_{IR,TOA})_{RAD} - Flux(\uparrow_{IR,TOA})_{CTL}) / Flux(\uparrow_{IR,TOA})_{CTL} \times 100\% \quad (5)$$

189 where, $Flux(\downarrow_{Solar,SFC})_{RAD}$, $Flux(\downarrow_{Solar,SFC})_{CTL}$ represents the downward solar
 190 radiation flux (w/m^2) at the surface of the RAD and CTL experiment.
 191 $Flux(\uparrow_{IR,TOA})_{RAD}$, $Flux(\uparrow_{IR,TOA})_{CTL}$ is the infrared radiation flux emitted from the
 192 Earth at TOA in the RAD and CTL experiments, respectively. Figure 2a
 193 displays the averaged ΔF_{SFC} at 06 UTC from 7 to 11 July. It can be seen that
 194 aerosol DRF decreased more than 15% of the solar radiation fluxes reaching
 195 the ground over most of China 3JNS Region and a decrease reaching up to
 196 20-25% in the most polluted area with the high AOD values. This result
 197 indicates the important impact of aerosol DRF on ground and near-ground
 198 radiation budgets. Figure 2b shows the mean ΔF_{TOA} of the 7-11 July, indicating
 199 that aerosol DRF reduced only 1-3% of infrared emission at the TOA during
 200 this haze episode, which is far lower than the surface downward solar
 201 radiation flux change. This result suggests that aerosol DRF has more
 202 important impacts on the ground and near-Earth surface radiation budgets,
 203 i.e., the PBL energy budget than on TOA.

204 **5. The radiative feedback on PBL meteorology due to aerosols**

205 The remarkable reforming of the surface and PBL radiation energy budget

206 by aerosols will certainly lead to changes in PBL thermodynamics, dynamics
207 and physical processes, which results in changes in PBL meteorological fields
208 and further the haze development. The impacts on air temperature,
209 turbulence distribution, PBLH, wind speed, air pressure, and PM2.5 due to
210 aerosols will be discussed, respectively, in the following section.

211 **5.1 The impacts on temperature**

212 The direct and initial change due to aerosols DRF is the temperature. It
213 can be seen that the surface temperature change reached up to -1 to -3 K at
214 06 UTC on 7-11 July (Fig. 3a) in the China 3JNS region corresponding to the
215 high AOD values and substantial negative values of surface SW flux changes
216 as shown in Figure1. A vertical cross-section of temperature was drawn along
217 latitude 38°N (black line in Fig. 3a) and it shows the vertical temperature
218 change due to aerosol DRF (Fig. 3b). Also shown is the reduction by aerosol
219 DRF of surface and PBL temperature over the land surface. A PBL
220 temperature decrease of 1 to 2K occurred over the China mainland (110-
221 118°E) and 0.5 to 1 K over the Korean peninsula (125-128°E), while the
222 aerosol impacts on the surface and PBL temperature changes were small or
223 increased weakly over the oceanic area. Over this cooling atmospheric layer
224 there existed a weak warming layer with a vertical height ranging from 975 to
225 600 hPa along latitude 38°N. The vertical sections of regional average
226 temperature change due to aerosols over LAND region (Fig. 3c), points A, B,
227 C, SEA1 and SEA2 areas (Fig. 3d) display the vertical temperature changes
228 over the China3JNS region with the highest pollution, China offshore, China
229 Sea, and the Japan Sea. It is clear from Figure 3c that temperature
230 diminished from the surface to about 850hPa over China 3JNS Region while
231 temperature increased above that level. This suggests the presence of
232 aerosol cooling effects on the PBL atmosphere and warming effects on the
233 atmosphere above it, which may lead to more stable stratification of the
234 atmosphere over this region. ~~Points A, B, and C lie offshore of the Chinese~~
235 ~~coast, their temperature changes and those within SEA1 (Fig. 3d) being quite~~
236 ~~different from those within the LAND region. Points A, B, and C lie offshore of~~
237 ~~the Chinese coast and SEA1 represents the near China Sea region. The~~

238 vertical profiles of temperature changing induced from aerosols' radiative
239 feedback effect over those are quite different from those over the LAND
240 region due to the different surface albedo and the height and depth of
241 aerosols layer. It can be seen from Figure 3d that aerosol heats the
242 atmosphere from the surface to a height of 600 hPa over these regions. This
243 is especially so in the PBL atmosphere because the higher aerosol layer and
244 the smaller AOD value may cause more unstable atmospheric stratification
245 over the sea areas. Aerosol DRF has little impact on the surface and PBL
246 temperatures in the SEA2 region, and only very weak warming can be found
247 above a height of 750 hPa owing to the further lower AOD values in this
248 region. The above results and the discussion on Figure 3 indicate that aerosol
249 DRF led to more stable atmospheric stratification over the China 3JNS Region
250 and to more unstable atmospheric stratification over offshore of China and the
251 China Sea regions during the haze episode of 7-11 July. This achieves an
252 important influence on local PBL meteorology and the regional atmosphere
253 circulation.

254 **5.2 The impacts on PBL turbulence diffusion**

255 Changes in regional atmospheric stratification positively results in varying
256 turbulence diffusion. The turbulence diffusion coefficient (FKTM) used in Part
257 1 of this study is a valid physical parameter that indicates the strength of
258 turbulence diffusion. Figure 4 displays FKTM changes due to aerosol DRF.
259 Figure 4a describes the regional distribution of mean impacts on turbulence
260 diffusion in the haze from 7 to 11 July and it can be seen that low turbulence
261 diffusion exists over the whole of 3JNS Region with mean FTKM values of 14-
262 45 m/g in the haze condition on 7-11 July 2008. Aerosol DRF led to a mean 5
263 m/g reduction of FTKM over most of the east China mainland and a lessening
264 of 10-15 m/g in China 3JNS Region, showing remarkable depression on the
265 local atmospheric turbulence diffusion process from aerosol DRF. Figure 4b
266 displays the daily changes in the regional averaged difference: $FKTM_{rad} -$
267 $FKTM_{ctl}$ over LAND and SEA1 in July 2008. It is clear from Figure 4b that
268 the averaged FKTM of the LAND region was reduced by aerosol DRF more or
269 less during the whole of July 2008. As with the haze event on 7-11 July, 2008,

270 the FKTM declined by about 7-9g/m and 8-10g/m during another haze
271 episode on 25-28 July, 2008, which was also initiated by aerosol DRF. FKTM
272 changes resulting from aerosol DRF also occurred over the SEA1 region but
273 these were small to negligible in scale. These results suggest that the
274 suppression of diffusion turbulence by aerosol DRF is both certain and
275 significant over the middle and eastern Chinese mainland with its high
276 pollutants while, in contrast, impact over the sea region is small and can be
277 negligible during haze episodes.

278 **5.3 The impacts on PBLH**

279 PBLH is another key parameter to describe the PBL features closely
280 related to haze and air pollution. Its impact on $PM_{2.5}$ and haze was discussed
281 in Part 1. Aerosol impacts on PBLH due to DRF during the haze episode on 7-
282 11 July are discussed in this section. Figure 5 shows PBLH changes due to
283 aerosol DRF. Figure 5a shows that the mean daytime PBLH was as low as
284 400-700m over the east China mainland during the haze episode on 7-11 July.
285 PBLH declined by about 50-300m generally in response to aerosol DRF over
286 this region; the difference between PBLH_{rad} and PBLH_{ctl} reaches up to
287 200-300m in China 3JNS Region. Figure 5b shows that daytime PBLH,
288 especially PBLH at local noon-time (06UTC), may have been diminished by
289 aerosol DRF evidently and steadily in July 2008, although its reduction varies
290 with time. The PBLH reduction may have reached to about 250 m on 10-11
291 July and 250-300m during another haze episode on 25-28 July. Figure 5b
292 also shows that aerosol DRF inflicts very weak impacts on PBLH over the sea
293 with increase or decrease PBLH slightly at different times.

294 **5.4 The impacts on PBL wind**

295 The influence of surface and PBL wind fields on haze pollution is as
296 important as, or even more important than, that of PBLH and diffusion
297 turbulence as discussed in Part 1, but the impact on PBL winds from aerosol
298 DRF is not so strong as its impact on PBLH and diffusion turbulence. PBL
299 wind changes due to aerosol DRF is minor and may be neglected when haze
300 pollution is weak. The focus is on the period from 9 to 11 July with the highest

301 PM_{2.5} and severest pollution to investigate the wind field changes due to
302 aerosol DRF. Figure 6a shows the difference of PBL averaged wind speed
303 between the RAD and CTL experiments (shading) and wind vector (contour)
304 of the CTL experiment. It can be seen from Figure 6a that the whole PBL wind
305 speed was increased by aerosol DRF over most of the middle and eastern
306 Chinese mainland region, while it declined over the offshore and sea areas.
307 Wind speed was increased from 0.4 to 0.8 m/s by aerosol DRF in certain
308 parts of China 3J Region with high particle concentration. Figure 6b also
309 indicates temporal changes in the LAND averaged wind speed difference
310 between the RAD and CTL experiments at the surface and PBL (950-850)
311 hPa from 00 UTC 9 to 00 UTC 12 July. Also shown is that both surface and
312 PBL wind speed was obviously increased by aerosol DRF over this period;
313 however, the extent of the increase in PBL wind speed was much greater than
314 in the case of the surface wind, indicating that aerosols may impose much
315 greater impacts on PBL winds than on surface winds.

316 **5.5 The impacts on the PBL air pressure pattern**

317 Figure 7a displays the PBL averaged air pressure pattern during 7 to 11
318 July from the CTL experiment. It can be seen that subtropical high pressure
319 controlled both the east China and China offshore regions. East China was
320 located in the west edge of the subtropical high with a weak southerly air flow
321 controlling this area. This air pressure pattern is conducive to retention of
322 haze (discussed in Part 1). The PBL averaged air pressure changes due to
323 aerosol DRF was calculated from the air pressure differences between the
324 RAD and CTL experiments. It can be seen from Figure7b that the whole PBL
325 air pressure was decreased by aerosol DRF over eastern China and its
326 downwind region, especially over the China offshore region, which resulted in
327 the obvious weakening of the subtropical high over China's offshore and sea
328 regions. The lessening and withdrawal eastward of the subtropical high
329 sustained the eastward-moving cold air from the northwest, which also
330 delivered a downward flow of cloud air together with some momentum from the
331 upper atmosphere to the PBL. This seems to have helped the breaking down
332 of the stable air pressure pattern that was controlling the retention of the haze.

333 **5.6 The impacts on surface PM_{2.5}**

334 The reforming of the local PBL meteorology structure by aerosol DRF, in
335 turn, impacts upon the PBL and surface PM_{2.5} spatial distribution, temporal
336 changes or, perhaps, the duration time of the haze. The radiative feedback on
337 PM_{2.5} by aerosols consists of the synthesized results from the PBL
338 meteorological parameters, involving temperature, turbulence diffusion, PBLH,
339 wind, air pressure and other items.

340 The averaged PM_{2.5} loading within the PBL (contour, kgm⁻²) of 7-11 July
341 in the CTL experiment has been calculated and shown in Figure 8 together
342 with the surface PM_{2.5} percentage changes attributable to aerosol DRF
343 (shaded). It can be seen that the aerosol DRF generally increases the surface
344 PM_{2.5} over east China, the percentage change being >10% over most of
345 China 3JNS region. The geographical location of the increasingly high
346 percentage of PM_{2.5} basically correlates with the location of the high PBL
347 PM_{2.5} loading. The PM_{2.5} increasing percentage by aerosol DRF can reach up
348 to more than 20% over the region with the highest PBL PM_{2.5} loading in China
349 3JNS Region. The result indicates that the higher the PBL PM_{2.5} loading, the
350 more PM_{2.5} might be concentrated at the surface due to aerosol DRF and in
351 terms of the averaged condition of the haze episode. Surface PM_{2.5} is
352 enhanced by about 10-20% due to aerosol DRF or even more over middle-
353 eastern China.

354 The temporal variations of surface PM_{2.5} of the China 3JNS region
355 averaged of the CTL and RAD experiments from 7 to 13 July are also
356 displayed and compared in order to evaluate the impacts of aerosol DRF (Fig.
357 9). It is shown that the aerosol DRF results in more PM_{2.5} particles
358 concentrating on the surface during the entire haze period from 05 GMT on 7
359 July to 18 GMT on July 11. If the surface PM_{2.5} concentration is regarded as
360 the indicator of haze pollution, it can also be seen that the obvious difference
361 of PM_{2.5} values between the CTL and RAD experiments during the period
362 from about 05 GMT on July 7 to about 18 GMT on July 11 and the LAND
363 mean surface PM_{2.5} also remains higher than 140ug/m³ during this period.
364 The difference of LAND mean surface PM_{2.5} between the CTL and RAD

365 experiments is small before or after that period and, at the same time, the
 366 PM_{2.5} values from both experiments are lower than 140ug/m³. This indicates
 367 that aerosol DRF may have very little impact on the haze sustaining period or
 368 keeping time of the haze episode because, when PM_{2.5} declines below a
 369 certain level, the aerosol DRF may not be efficient enough to change the PBL
 370 meteorological circulation and then reform the PM_{2.5} spatial and temporal
 371 distribution.

372 The responses of PBL meteorology quantities to aerosol DRF relates,
 373 on the one hand, to the perturbation strength from aerosols and, on the other
 374 hand, to their thermodynamics and dynamic characteristics of these
 375 meteorological entities. In order to evaluate and order the sensitivity of these
 376 parameters to aerosol DRF, a weighting coefficient g_i is defined as follows:

$$377 \quad g_{i_LAND} = \frac{\text{var}(i)_{rad_LAND} - \text{var}(i)_{ctl_LAND}}{\text{var}(i)_{ctl_LAND}} \quad (6)$$

378 where, $\text{var}(i)$ stands for different meteorological variables involving radiation
 379 fluxes, wind speed, PBLH, FKTM, and PM_{2.5}. The subscript *ctl* and *rad* identify
 380 the CTL and RAD experiments. The subscript LAND means that all the
 381 variables are the mean values of the LAND region averaged and stand for the
 382 mean condition of China 3JNS Region. With regard to air temperature and air
 383 pressure, the zero values have no physical meaning and g_i is not calculated
 384 here and only the changes due to aerosol DRF are listed. Table 1 lists the
 385 daily g_i from 7 to 11 and the averaged g_i of the haze episode on 7-11 July. It
 386 can be seen, therefore, that the response of the meteorological parameters to
 387 aerosol DRF from high to low is FKTM, PBLH, ΔF_{SFC_Solar} , PBL wind, and
 388 ΔF_{TOA} . The process averaged g_{fkfm} for 7-11 July is -0.54 daily ranging from -
 389 0.40 to -0.62 and g_{PBLH} is -0.33 ranging from -0.29 to -0.39, showing that the
 390 most important impacting mechanism from aerosol DRF is the suppression of
 391 PBL turbulence diffusion, which may lead to increasing the surface PM_{2.5} and
 392 to positive radiative feedback to haze pollution. g_{wind} is 0.09 with daily values
 393 ranging from 0.01 to 0.16. The PBL air pressure at 06 UTC fell to a mean of

394 15 hPa for the period 7-11 July and ranged from 0.12 to 0.16, which
395 weakened the subtropical high. Both the changes in wind and air pressure
396 may result in negative feedback to haze development. Comparing g_{wind} with
397 g_{fktm} and g_{PBLH} indicates that aerosol DRF may impose more important
398 impacts on PBL height and turbulence diffusion than its impacts on PBL wind
399 and air pressure. The mean $g_{pm2.5}$ is 0.13 for the 7-11 July period ranged from
400 0.10 to 0.16 and resulted from the synthesized influence of the two opposing
401 sides, as mentioned above, showing the final positive feedback of surface
402 $PM_{2.5}$ and haze pollution from aerosol DRF. $g_{flux_sw_sfc}$ is the weighing
403 coefficient of change in downward solar radiation flux due to aerosols and a
404 mean value of 0.18 ranging from 0.14 to 0.20. The weighing coefficient of
405 changing TOA longwave radiation ($g_{flux_lw_TOA}$) is the smallest with a value of
406 0.02, showing that total impacts on regional TOA from aerosol DRF are minor
407 and may be neglected during haze episodes.

408 **6. Discussion and conclusion**

409 Focusing on a haze episode from 7 to 11 July 2008, two model
410 experiments (the control experiment (CTL) without calculation of aerosol-
411 radiation effects and the RAD experiment with online calculating aerosol-
412 radiation interaction) are designed to evaluate aerosol direct radiative effects
413 and feedbacks on the regional PBL atmospheric circulation related to haze
414 formation in general and the specific haze episode in July, 2008. The study
415 involves impacts on surface SW and TOA outgoing radiation flux, temperature,
416 PBL turbulence diffusion, wind, PBLH, air pressure pattern and $PM_{2.5}$. A
417 detailed discussion is summarized as follows:

418 Solar radiation flux reaching the ground is decreased by about 15%
419 generally in China 3JNS Region and by 20-25% in the region with the highest
420 AOD. Only 1-3% of longwave outgoing flux is decreased at the TOA. Aerosol
421 DRF has a greater impact on the ground and near surface radiation budget
422 than in the upper atmosphere. Aerosol cools the lower PBL or the whole PBL,
423 while warming the upper PBL or the atmosphere above it, which leads to
424 stable stratification of the atmosphere over the middle and eastern Chinese
425 region. In contrast, aerosol heats the PBL atmosphere weakly causing

426 unstable atmospheric stratification over the Chinese offshore area. On the
427 one hand, aerosol DRF suppresses diffusion turbulence and decrease PBLH
428 significantly over the China 3JNS Region, which enhances particle
429 concentration on the PBL and the surface intensifying the haze formation. On
430 the other hand, aerosol DRF increases PBL wind speed and weakens
431 subtropical high pressure which contributes to the collapsing of haze pollution
432 over this region. The impacts from the two opposite effects ultimately result in
433 an averaged increase of 10-20% in surface $PM_{2.5}$ over the China 3JNS region
434 by aerosol DRF, but no change in the persistence time of the haze pollution.
435 The ranking order of the impacts on meteorological parameters due to aerosol
436 DRF according to the weighting coefficient is the turbulence diffusion, PBLH,
437 short wave radiation flux at the surface, $PM_{2.5}$, PBL wind and the TOA
438 longwave outgoing flux when air temperature and air pressure are not
439 considered.

440 Given that the most discussions above are based on a single case of
441 haze that occurred on 7-11 July 2008, there is clearly a need for research into
442 more summer-time haze episodes in order to support the conclusions. As
443 haze pollution episodes occur very frequently in autumn and winter in east
444 China, the PBL meteorological condition, the chemical composition of
445 aerosols and the optical characteristics are quite different from those in
446 summer and so is the radiative feedback. Finally, it should be noted that the
447 response of different meteorological fields to aerosol DRF and their
448 contributions to regional circulation changes also relate to their dynamic
449 thermodynamic features.

450 **Acknowledgments:**

451 **This work is supported by the National Basic Research Program**
452 **(973) (2011CB403404), the National Natural Scientific Foundation of**
453 **China (Nos. 41275007&41130104), and the CAMS key projects (Nos.**
454 **2013Z007).**

455

456 **References:**

- 457 Chapman, E. G., Gustafson Jr., W. I., Easter, R. C., Barnard, J. C., Ghan, S.
458 J., Pekour, M. S., and Fast J. D: Coupling aerosol-cloud-radiative
459 processes in the WRF-Chem model: Investigating the radiative impact of
460 elevated point sources, *Atmos. Chem. Phys.*, 9, 945–964, 2009.
- 461 Che, H., Zhang, X. Y., Li, Y., Zhou, Z. and Qu, J. J.: Horizontal visibility trends
462 in China 1981-2005, *Geophysical Research Letters*, 34, L24706,
463 doi:10.1029/2007GL031450, 2007.
- 464 Che, H., Yang, Z. F., Zhang, X. Y., Zhu, C., Ma, Q. L., Zhou, H.G., and Wang.,
465 P.: Study on the Aerosol Optical Properties and their Relationship with
466 Aerosol Chemical Compositions over three Regional Background stations
467 in China, *Atmospheric Environment*, 43(5),1093-1099, 2009.
- 468 Che, H., Xia, X., Zhu, J., Li, Z., Dubovik, O., Holben, B., Goloub, P., Chen, H.,
469 Estelles, V., Cuevas-Agulló, E., Blarel, L., Wang, H., Zhao, H., Zhang, X.,
470 Wang, Y., Sun, J., Tao, R., Zhang, X., and Shi, G.: Column aerosol optical
471 properties and aerosol radiative forcing during a serious haze-fog month
472 over North China Plain in 2013 based on ground-based sunphotometer
473 measurements, *Atmos. Chem. Phys.*, 14, 2125-2138, doi:10.5194/acp-14-
474 2125-2014, 2014.
- 475 Cheng, Y., Canuto, V. M., and Howard, A. M.: An improved model for the
476 turbulent PBL, *J. Atmos. Sci.*, 59, 1550–1565, 2002.
- 477 Chou, M. D., Suarez, M. J., Ho, C. H., Yan, M. M. H., and Lee, K. T.:
478 Parameterizations for Cloud Overlapping and Shortwave Single-
479 Scattering Properties for Use in General Circulation and Cloud Ensemble
480 Models, *J. Clim.*, 11, 202–214, 1998.
- 481 Chou, M. D., Suarez, M. J., Liang, X. Z., and Michael M.-H. Y.: A Thermal
482 Infrared Radiation Parameterization for Atmospheric Studies, Technical
483 Report Series on Global Modeling and Data Assimilation, NASA/TM-
484 2001-104606, 19, America, Goddard Space Flight Center, Greenbelt,
485 Maryland, 55, 2001.
- 486 Fast, J. D., Gustafson, Jr., W. I., Easter, R. C., Zaveri, R. A., Barnard, J. C.,
487 Chapman, E. G., Grell, G. A., and Peckham, S. E.: Evolution of Ozone,
488 Particulates and Aerosol Direct Radiative Forcing in the Vicinity of
489 Houston Using a Fully Coupled Meteorology-Chemistry-Aerosol Model, *J.*

490 Geophys. Res., 111, D21305, doi:10.1029/2005JD006721, 2006.

491 Grell, G. A., Peckham, S. E., Schmitz, R., McKenn, S. A., Frost, G.,
492 Skamarock, W. C., and Eder, B.: Fully Coupled “Online” Chemistry within
493 the WRF Model, *Atmos. Environ.*, 39, 6957–6975, 2005.

494 Hansen, J., Sato, M., and Ruedy, R.: Radiative Forcing and Climate
495 Response, *J. Geophys. Res.*, 102, 6831–6864, 1997.

496 Heinold, B., Tegen, I., Schepanski, I., K., and Hellmuth, O.: Dust radiative
497 feedback on Saharan boundary layer dynamics and dust mobilization,
498 *Geophys. Res. Lett.*, 35, L20817, doi:10.1029/2008GL035319, 2008.

499 Huang, J., P. Minnis, B. Lin, T. Wang, Y. Yi, Y. Hu, S. Sun-Mack, and K.
500 Ayers, Possible influences of Asian dust aerosols on cloud properties and
501 radiative forcing observed from MODIS and CERES, *Geophys. Res. Lett.*,
502 33 (6), L06824, doi:10.1029/2005GL024724, 2006a.

503 Huang, J., Lin, B., Minnis, P., Wang, T., Wang, X., Hu, Y., Yi, Y., and Ayers, J.:
504 Satellite-based assessment of possible dust aerosols semi-direct effect on
505 cloud water path over East Asia, *Geo. Res. Lett.*, 33 (19), L19802,
506 doi:10.1029/2006GL026561, 2006b.

507 Huang, J., Minnis, P., Yi, Y., Tang, Q., Wang, X., Hu, Y., Liu, Z., Ayers, K.,
508 Trepte, C., and Winker D.: Summer dust aerosols detected from
509 CALIPSO over the Tibetan Plateau, *Geophys. Res. Lett.*, 34(18), L18805,
510 doi:10.1029/2007GL029938, 2007.

511 Huang, J.*, P. Minnis, B. Chen, Z. Huang, Z. Liu, Q. Zhao, Y. Yi, and J. Ayers,
512 Long-range transport and vertical structure of Asian dust from CALIPSO
513 and surface measurements during PACDEX, *J. Geophys. Res.*, 113 (D23)
514 2008, D23212, doi:10.1029/2008JD010620, 2008.

515 Huang, J., Fu, Q., Su, J., Tang, Q., Minnis, Y., Hu, P., Yi, Y., and Zhao, Q.:
516 Taklimakan dust aerosol radiative heating derived from CALIPSO
517 observations using the Fu-Liou radiation model with CERES constraints,
518 *Atmos. Chem. Phys.*, 9 (12), 2009.

519 Li, Z. Q., Xia, X. A., Cribb, M., Mi, W., Holben, B., Wang, P. C., Chen, H. B.,
520 Tsay, S. C., Eck, T. F., Zhao, F. S., Dutton, E. G., Dickerson, R. E.:
521 Aerosol optical properties and their radiative effects in northern China. *J.*
522 *Geophys. Res.* 112(11): D22S01, doi10.1029/2006JD007382, 2007.

523 Liao, H., Chen, W. T., and Seinfeld, J. H.: Role of climate change in global

524 predictions of future tropospheric ozone and aerosols, *J. Geophys. Res.*,
525 111, D12304, doi:10.1029/2005JD006852, 2006.

526 Perez, C., S. Nickovic, G. Pejanovic, J. M. Maldasano, and E. Ozsoy (2006),
527 Interactive dust-radiation modeling: A step to improve weather forecast, *J.*
528 *Geophys. Res.*, 111(D16206), doi:10..1029/2005JD006717.

529 Pleim, J., 2007b: A combined local and non-local closure model for the
530 atmospheric boundary layer. Part II: Application and evaluation in a
531 mesoscale meteorological model. *J. Applied Meteor. Climatology*, 46,
532 1396–1409.

533 Ramanathan, V., Crutzen, P. J., Kiehl, J. T., and Rosenfeld, D.: Aerosols,
534 Climate and the Hydrological Cycle, *Science*, 294, 2119–2124, 2001.

535 Santanello Jr., J. A., Friedl, M. A., and Kustas, W. P.: An empirical
536 investigation of convective planetary boundary layer evolution and its
537 relationship with the land surface, *J. Applied Meteor.*, 44, 917–932,2005.

538 Shindell, D. and Faluvegi, G.: Climate response to regional radiative forcing
539 during the twentieth century, *Nat. Geosci.* 2, 294–300,
540 doi:10.1038/ngeo473, 2009.

541 Voogelezang, D. H. P., and Holtslag, A. A. M.: Evaluation and model impacts of
542 alternative boundary-layer height formulations, *Bound.-Layer Meteor.*, 81,
543 245-269, doi:10.1007/BF02430331, 1996.

544 Wang, J., and Christopher, A.: Mesoscale modeling of Central American
545 smoke transport to the United States: 2. Smoke radiative impact on
546 regional surface energy budget and boundary layer evolution, *J. Geophys.*
547 *Res.*, 111, D14S92, doi:10.1029/2005JD006720, 2006.

548 Wang, H., Gong, S. L., Zhang, H. L., Chen, Y., Shen, X. S., Chen, D. H., Xue,
549 J. S., Shen, Y. F., Wu, X. J., and Jin, Z. Y.: A new-generation sand and
550 dust storm forecasting system GRAPES_CUACE/Dust: Model
551 development, verification and numerical simulation, *Chin. Sci. Bull*, 55(7),
552 635-649, doi: 10.1007/s11434-009-0481-z, 2010.

553 Wang, H., Zhang, X. Y., Gong, S., Chen, Y., Shi, G., and Li, W.: Radiative
554 feedback of dust aerosols on the East Asian dust storms, *J. Geophys.*
555 *Res.*, 115, D23214, doi:10.1029/2009JD013430, 2010.

556 Wang, H., Shi, G. Y., Zhu, J., Chen B., Che, H., and Zhao T. L.: Case study of
557 longwave contribution to dust radiative effects over East Asia. *Chin Sci*

558 Bull, 30, 3673-3681, doi:10.1007/s11434-013-5752-z, 2013
559 Wang H., Tan, S. C., Wang, Y., Jiang, C., Shi, G. Y., Zhang M., Che, H. Z.: A
560 multisource observation study of the severe prolonged regional haze
561 episode over eastern China in January 2013, Atmos. Environ., 89, 807-
562 815, 2014.

563 Yu, H., Kaufmann, Y. J., and Chin, M., et al.: A Review of Measurement-
564 Based Assessments of the Aerosol Direct Radiative Effect and Forcing,
565 Atmos. Chem. Phys., 6, 613–666, 6, 613–666, doi:110.5194/acp-6-613-
566 2006
567 , 2006.

568 Zhang X. Y., Sun, J. Y., and Wang, Y. Q., et al.: Factors contributing to haze
569 and fog in China, Chin. Sci. Bull. (Chin Ver), 58,1178–1187, doi:
570 10.1360/972013-150,2013.

571
572
573
574
575
576
577
578
579
580
581

582 | Table 1 caption

583 Table 1 Weighing coefficient of the response of meteorological parameters to aerosol DRF

Time (DD:HH)	g _{flux_sw_sfc}	g _{flux_lw_toa}	DT ₀₆ (K)	g _{difu}	g _{wind_PBL}	g _{PBLH}	DP ₀₆ (hPa)	g _{PM25}
7:00-7:24 UTC	-0.14	-0.01	-0.93	-0.40	0.01	-0.30	-16	0.10
8:00-8:24 UTC	-0.18	-0.02	-1.02	-0.48	0.03	-0.29	-14	0.14
9:00-9:24 UTC	-0.18	-0.02	-1.20	-0.57	0.15	-0.31	-12	0.16
10:00-10:24 UTC	-0.20	-0.03	-1.13	-0.62	0.16	-0.39	-14	0.15
11:00-11:24 UTC	-0.18	-0.02	-0.6	-0.54	0.11	-0.36	-14	0.11
Averaged	-0.18	-0.02	-0.98	-0.52	0.09	-0.33	-15	0.13

584

585

586

587

588

589

590 Captions to Figures

591 Fig.1 The averaged MODIS (top) and modeled AOD (bottom) of 7-11 July
592 2008: LAND represents the polluted area in the China 3JNS Region; points A,
593 B, and C represent China offshore; domains SEA1 and SEA2 refer for China's
594 Huang Sea and the Sea of Japan

595 Fig. 2 The change percentage in the surface SW flux at 06 UTC (a) and in
596 TOA outgoing LW flux (b) due to aerosol DRF during the 7-11 July period

597 Fig. 3 Mean temperature changes (K) at 06 UTC of 7-11 July due to aerosol
598 DRF: (a) surface temperature; (b) vertical section at 38°N of (a); (c) vertical
599 section of domain LAND region; (d) vertical section of points A, B, C, SEA1
600 and SEA2.

601 Fig. 4 FKTM change (m/s) due to aerosol DRF: (a) Mean FKTM by the CTL
602 experiment (shaded) and FKTM difference between the RAD and CTL
603 experiments (contour) of 7-11 July; (b) Daily changes of LAND and SEA1
604 averaged FKTM_rad-FKTM_ctl at the surface from 1 to 31, July.

605 Fig. 5 PBLH changes (m) due to aerosol DRF: (a) Daytime mean PBLH of the
606 CTL experiment (contour) and its difference between the RAD and CTL
607 experiments (shading) of 7-11 July; (b) LAND and SEA1 averaged PBLH
608 difference between the RAD and CTL experiments from 1 to 31 July, 2008.

609 Fig. 6 Wind field changes (m/s) due to aerosol DRF: (a) The mean PBL wind
610 vector of CTL experiment (contour) and PBL averaged wind speed difference
611 between the RAD and CTL experiments (shading) of 9-11 July. (b) Temporal
612 changes of LAND averaged wind speed difference between the RAD and CTL
613 experiments at the surface and 950-850 hPa height from 9 to 11 July.

614 Fig. 7 The PBL averaged air pressure (hPa) from the CTL experiment
615 (uppertop) and its difference between the RAD and CTL experiments (bottom)
616 of 7-11 July.

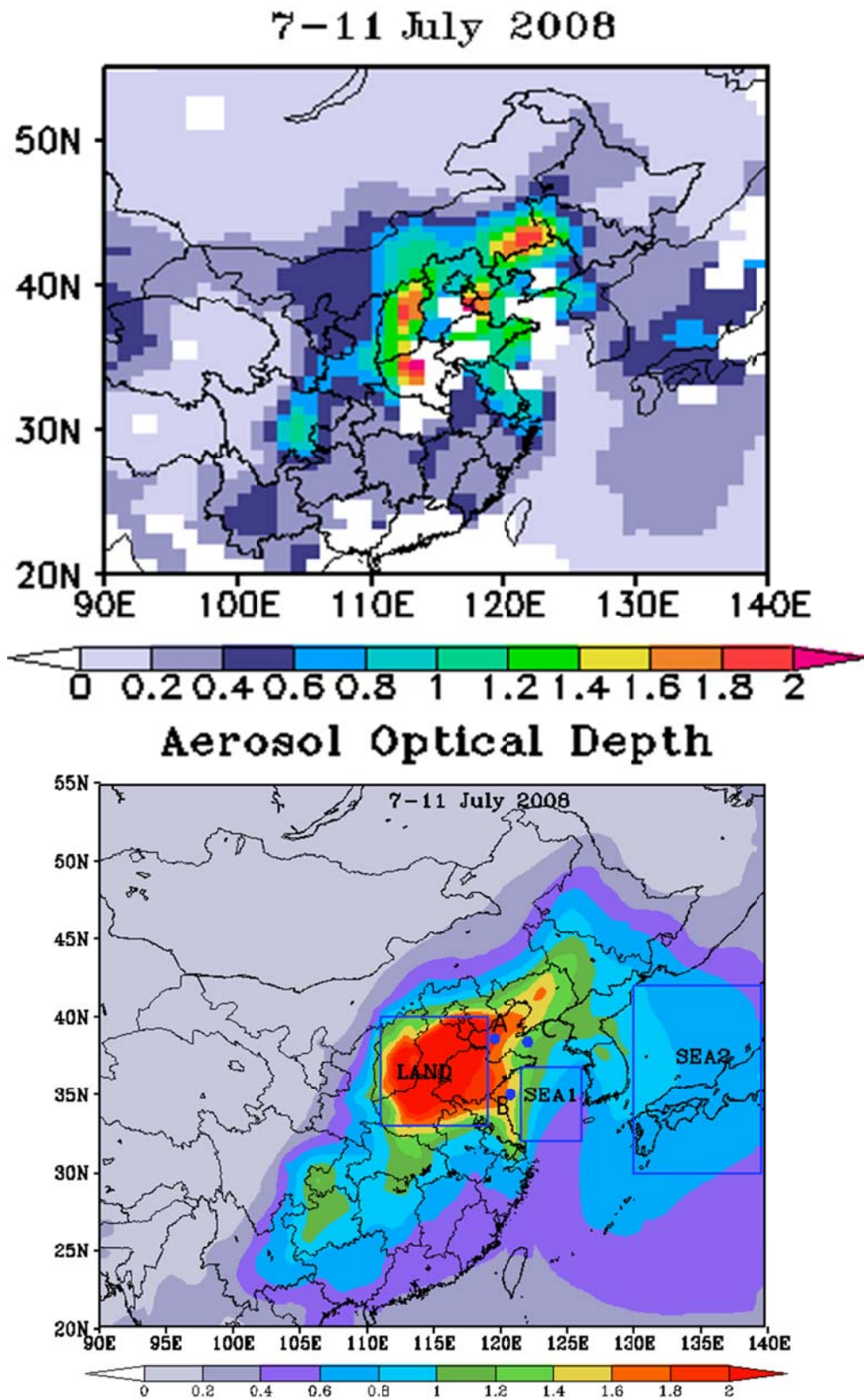
617 Fig. 8 The averaged PM2.5 loading within the PBL (contour, kg/m²) for 7-11
618 July of the CTL experiment and the surface PM2.5 change percentage due to
619 aerosol DRF for 7-11 July (shaded).

620 Fig. 9 Temporal changes of Land averaged surface PM2.5 by the CTL and

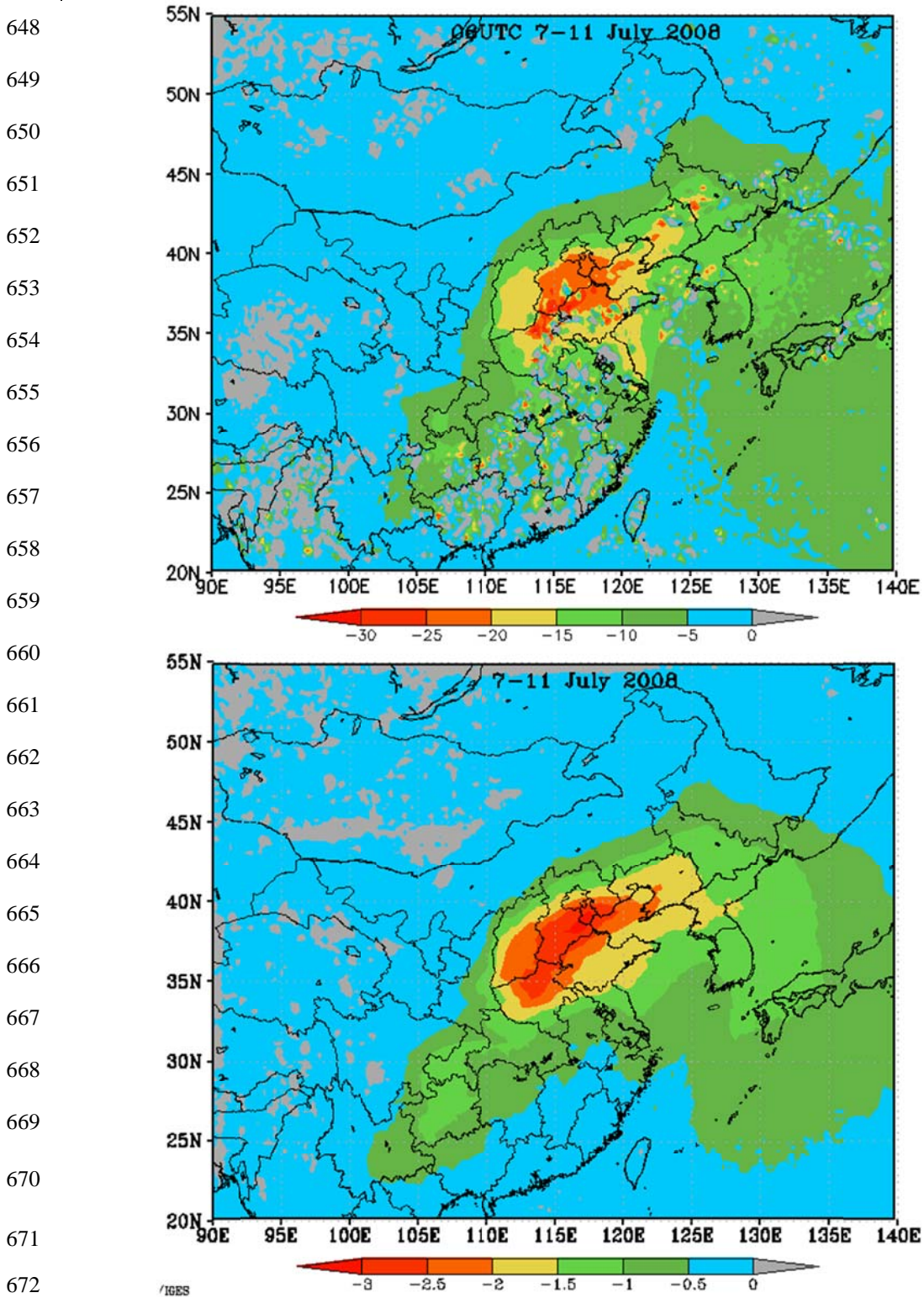
621 RAD experiments

622

627 Fig.1 The averaged MODIS (top) and modeled AOD (bottom) of 7-11 July
 628 2008: LAND represents the polluted area in the China 3JNS Region; points A,
 629 B, and C represent China offshore; domains SEA1 and SEA2 refer for China's
 630 Huang Sea and the Sea of Japan

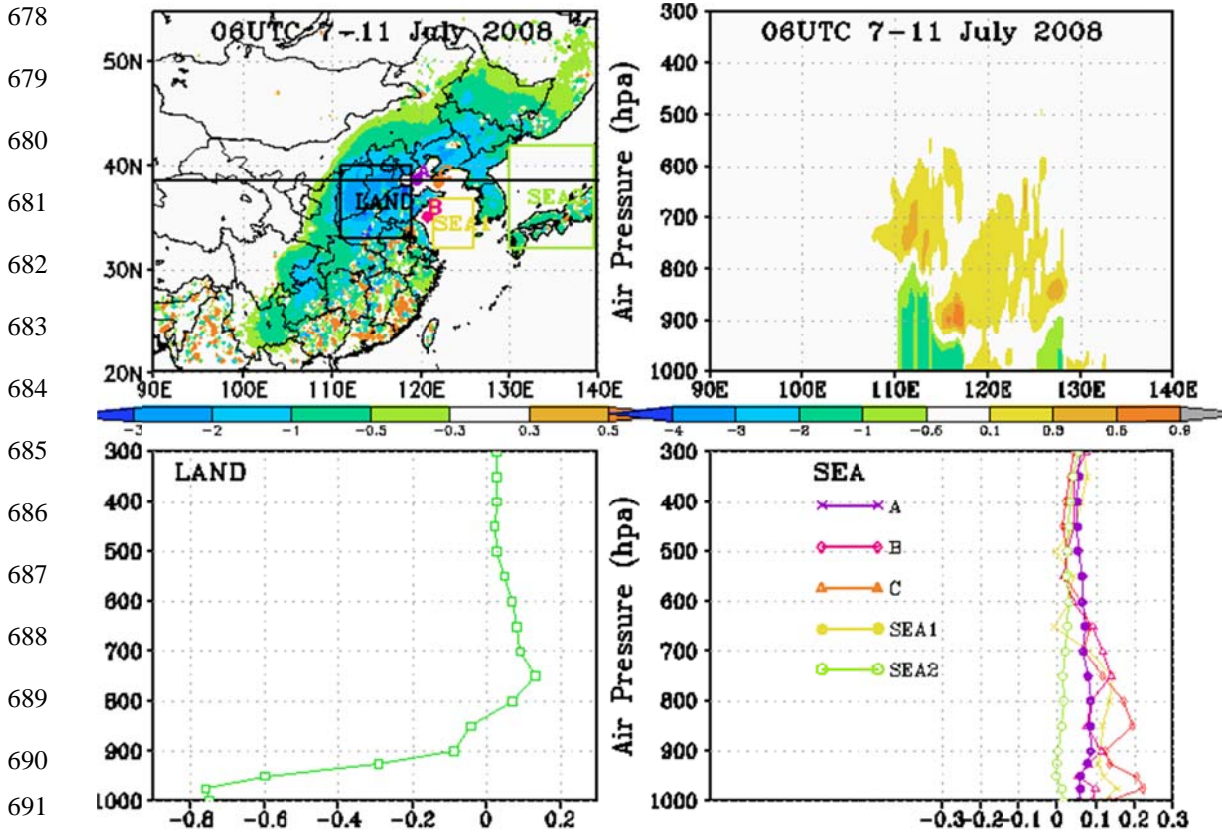


647 Fig. 2 The change percentage in the surface SW flux at 06 UTC (a) and in
648 TOA outgoing LW flux (b) due to aerosol DRF during the 7-11 July period.

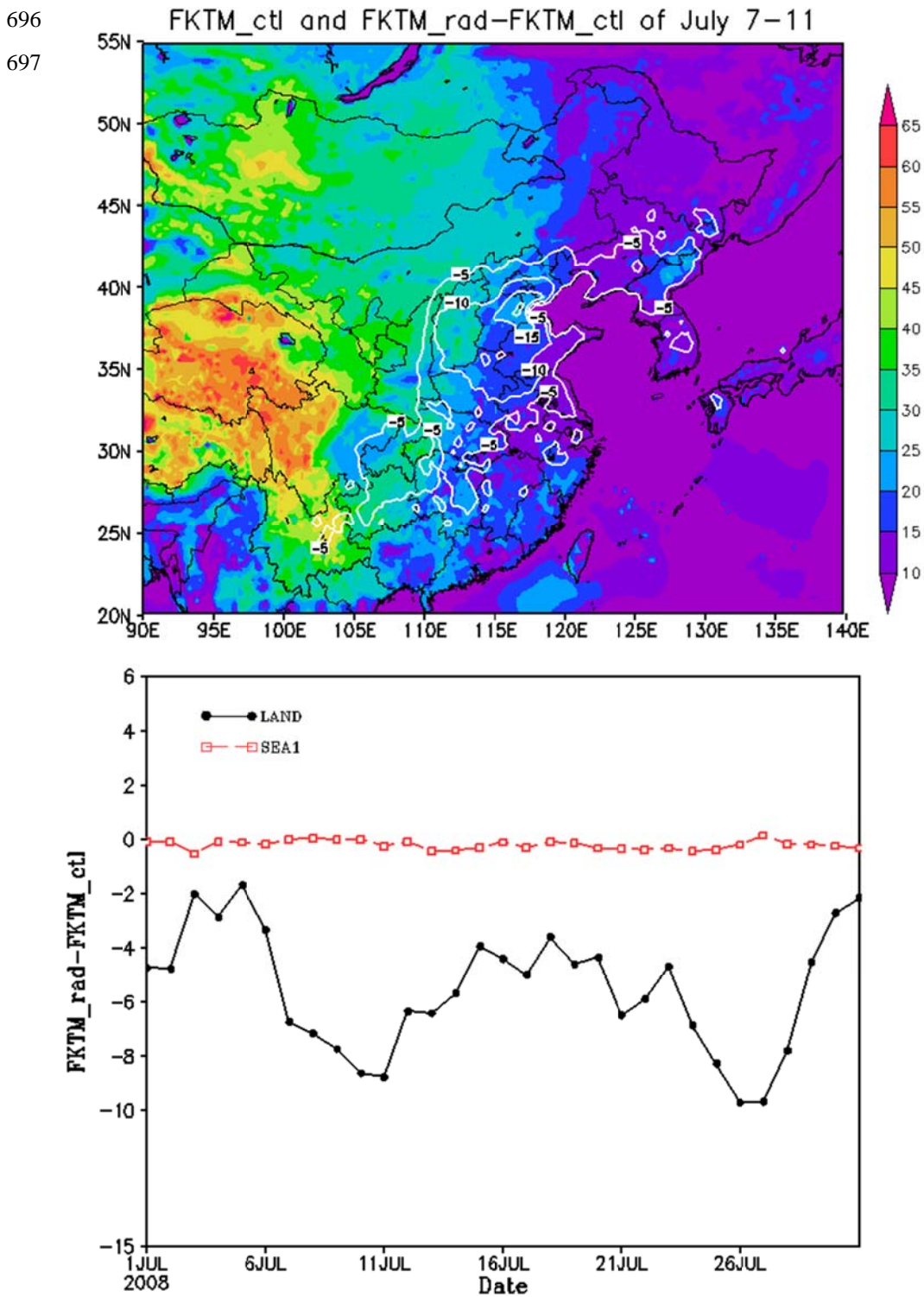


673

677 Fig. 3 Mean temperature changes (K) at 06 UTC of 7-11 July due to aerosol
678 DRF: (a) surface temperature; (b) vertical section at 38°N of (a); (c) vertical
679 section of domain LAND region; (d) vertical section of points A, B, C, SEA1
680 and SEA2.

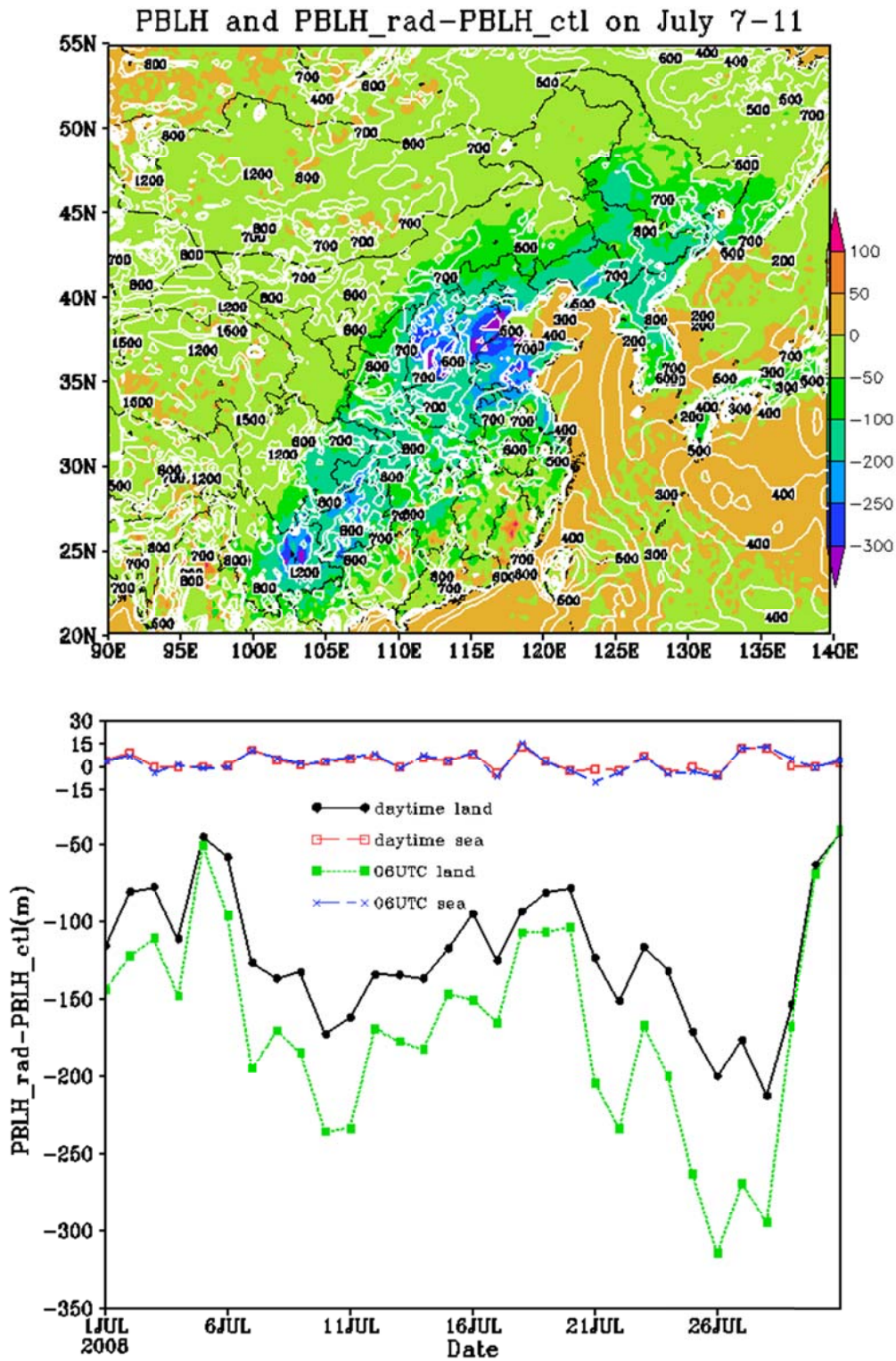


695 Fig. 4 FKTM change (m/s) due to aerosol DRF: (a) Mean FKTM by the CTL
 696 experiment (shaded) and FKTM difference between the RAD and CTL
 697 experiments (contour) of 7-11 July; (b) Daily changes of LAND and SEA1
 698 averaged $FKTM_{rad}-FKTM_{ctl}$ at the surface from 1 to 31, July.



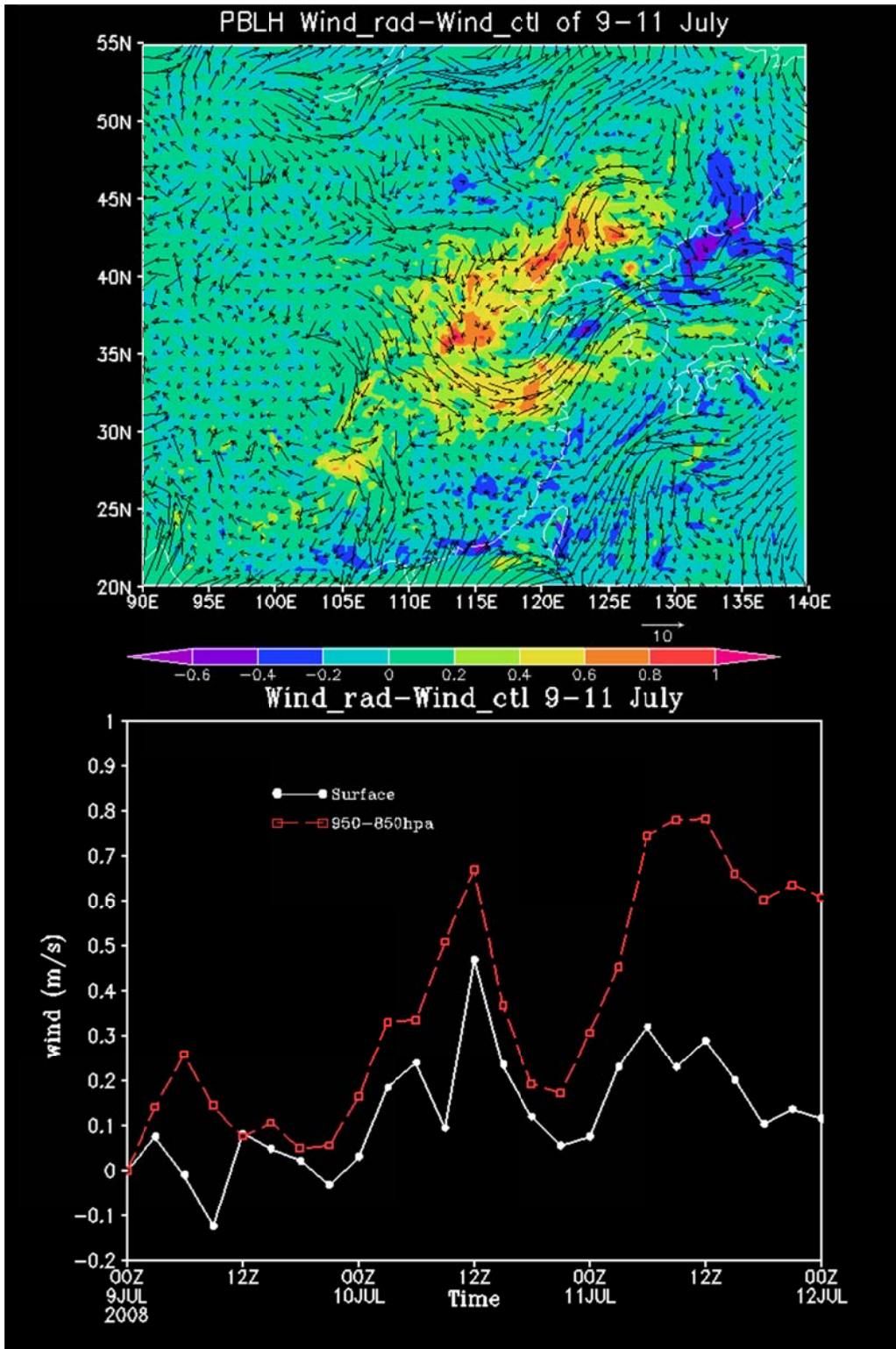
701 Fig. 5 PBLH changes (m) due to aerosol DRF: (a)Daytime mean PBLH of the
 702 CTL experiment (contour)and its difference between the RAD and CTL
 703 experiments (shading) of7-11 July; (b)LAND and SEA1 averaged PBLH
 704 difference between the RAD and CTL experiments from 1 to 31 July, 2008.

702
 703
 704
 705
 706
 707
 708
 709
 710
 711
 712
 713
 714
 715
 716

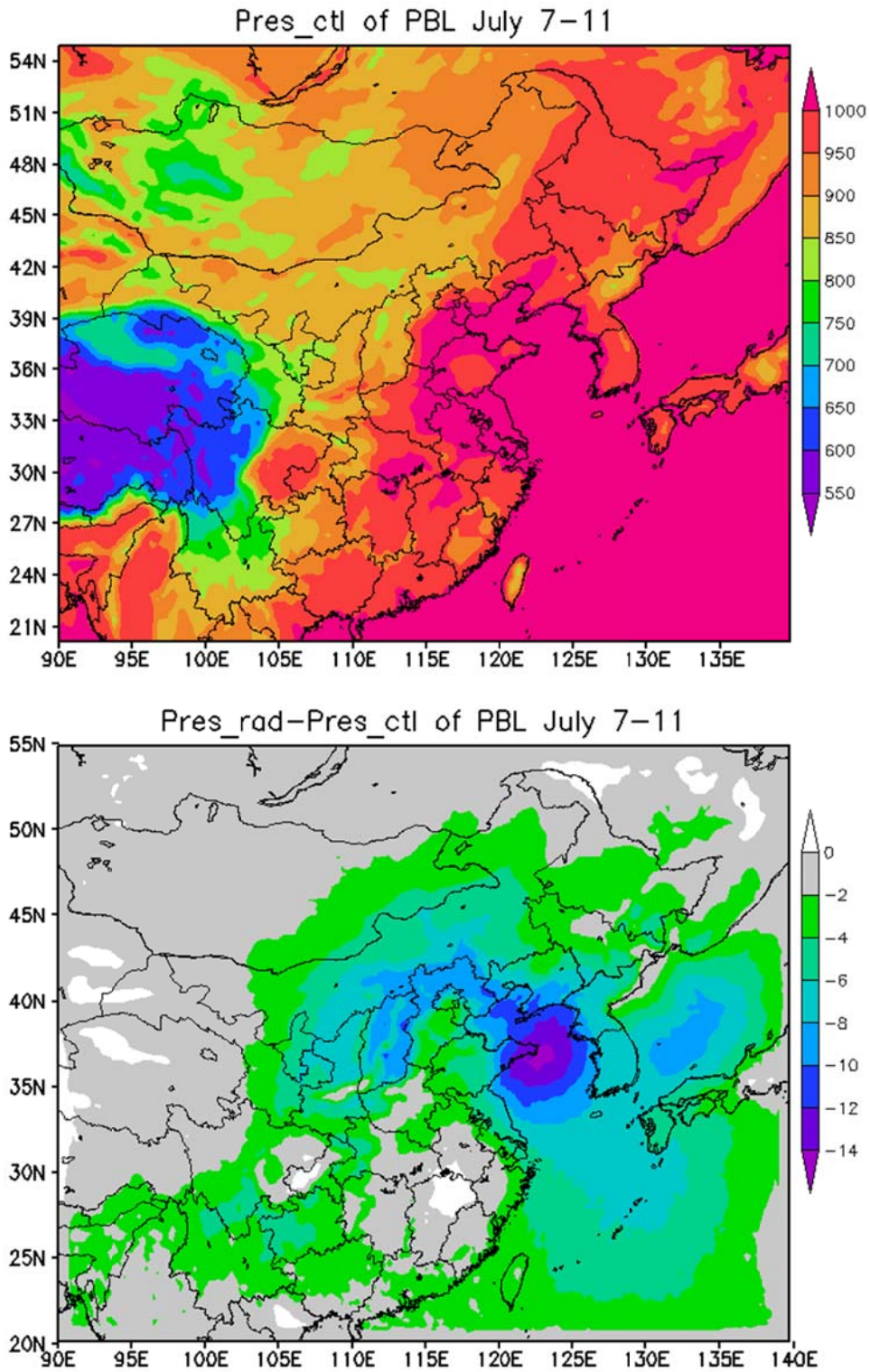


722 Fig. 6 Wind field changes (m/s) due to aerosol DRF: (a) The mean PBL wind
 723 vector of CTL experiment (contour) and PBL averaged wind speed difference
 724 between the RAD and CTL experiments (shading) of 9-11 July. (b)
 725 Temporal changes of LAND averaged wind speed difference between the
 726 RAD and CTL experiments at the surface and 950-850 hPa height from 9 to
 727 11 July.

723
 724

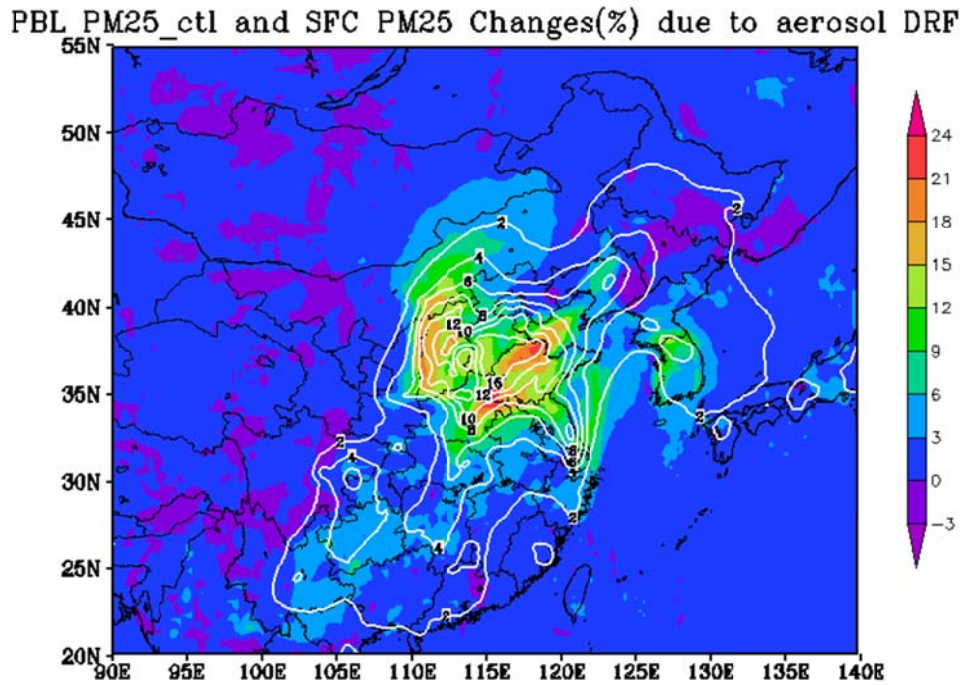


727 | Fig. 7 The PBL averaged air pressure (hPa) from the CTL experiment (top)
728 | and its difference between the RAD and CTL experiments (bottom) of 7–11
729 | July.
728

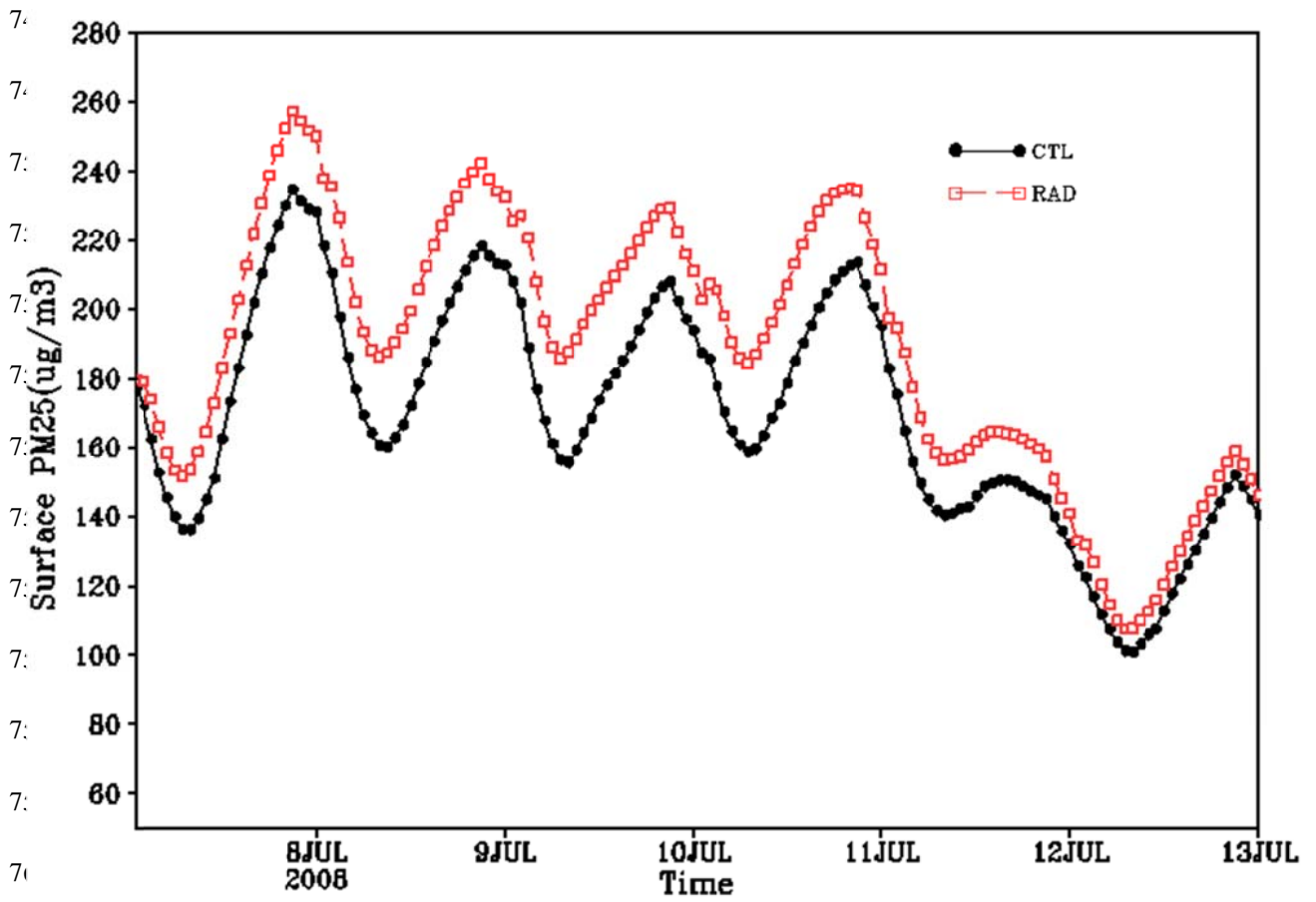


731 Fig. 8 The averaged $PM_{2.5}$ loading within the PBL (contour, kg/m^2) for 7-11
732 July of the CTL experiment and the surface $PM_{2.5}$ change percentage due to
733 aerosol DRF for 7-11 July (shaded)

732
733
734
735
736
737
738
739
740
741
742
743
744
745



747 Fig. 9 Temporal changes of Land averaged surface PM2.5 by the CTL and
748 RAD experiments



761
762
763